INTERACTIONS OF VOLTAGE-SENSING DYES WITH MEMBRANES

I. STEADY-STATE PERMEABILITY BEHAVIORS INDUCED BY CYANINE DYES

S. KRASNE, *Department of Physiology, Ahmanson Neurobiology Laboratory, and Molecular Biology Institute, University of California, Los Angeles, California 90024 U.S.A.*

ABSTRACT The effects of a series of thiadicarbocyanine dyes, $diSC_n(5)$, in altering the electrical properties of lipid bilayer membranes have been studied as a function of the membrane's intrinsic surface-charge density, the aqueous ionic strength, and the length (n) of the hydrocarbon side chains on the dye. Zero-current conductances, transmembrane potentials, and conductance-voltage relationships induced by these dyes were measured. All dyes studied altered membrane permeability properties; however these alterations were much larger at lower (e.g. 10^{-3} M) than at higher (e.g. 10^{-1} M) ionic strengths. The data suggest that such perturbations would not be troublesome for most biological preparations in which these dyes have been studied. The mechanisms by which these dyes alter membrane permeabilities vary in going from short-chained to long-chained dyes, the former forming voltage-gated, ion-permeant pores and the latter acting predominantly as anion carriers (forming 2:1 dye-anion complexes). In the case of $diSC_3(5)$, the predominant mechanism of altering membrane permeabilities changes in going from neutral to negatively charged membranes and also depends upon aqueous ionic strength and dye concentration.

INTRODUCTION

Over the last few years a number of dyes have been discovered which give large absorbance or fluorescence changes in response to changes in the voltage difference across membranes of cells, organelles, and lipid vesicles (see reviews by Waggoner, 1976; Cohen and Salzberg, 1978). These "optical probes" offer the possibility of monitoring changes in membrane potentials in cells and organelles too small to impale with microelectrodes and in cellular networks in which the individual cells are too numerous to monitor by standard electrophysiological techniques. These dyes can be divided into two classes. Dyes in the first class, which have been termed "slow-responding" dyes, give large signals in response to slow changes, but small signals in response to rapid changes, in the transmembrane potential; thus these dyes serve as particularly useful monitors in cell, organelle, and vesicle suspensions. Dyes in the second class, which have been termed "fast-responding" dyes, give much larger signals in response to rapid changes in the transmembrane potential than do the slow-responding dyes; these dyes are promising as monitors of action potentials in excitable cells and subcellular structures and of the kinetics of transmembrane potential changes.

The present series of papers will focus upon cyanine-, oxonol-, and merocyanine-based dyes because the optical responses of these dyes to transmembrane-potential changes are much larger than other dyes that have been studied (Cohen et al., 1974; Waggoner, 1976). Much work has already been published characterizing the relative sensitivities of these dyes to transmembrane-potential changes in a variety of preparations and demonstrating that the optical responses of these dyes do indeed follow the transmembrane-potential difference. For recent reviews of this body of literature, the reader is referred to Waggoner (1976) and to Cohen and Salzberg (1978). Relatively little has been published on the manner in which these dyes interact with membranes, whether they alter intrinsic membrane properties (e.g. permeabilities, surface potentials, fluidity), and how variations in membrane structure, aqueous composition, or dye structure alter these interactions. (A notable exception for cyanine and oxonol dyes is the work of Waggoner et al., 1977, which is discussed below. For naphthylamine dyes, some such studies have been reported by McLaughlin and Harary [1976] and by Haynes and Simkowitz [1977].) The present series of papers attempts such an investigation, using Mueller-Rudin-style, lipid-bilayer membranes and liposomes to characterize these dye-membrane interactions.

The first two papers examine the interactions of a series of cyanine dyes, classified as slow-responding dyes, with neutral and negatively charged bilayer membranes. The structures of the dyes studied and the terminologies used to designate them are illustrated in Fig. 1. The series of (positively charged) dyes, $diSC_n(5)$, was studied because, according to Waggoner (1976), "... $diSC_3(5)$ is presently the best dye for measuring membrane potentials of cells, organelles, and vesicles in suspension...." The present paper describes the steady-state, zero-current conductances, transmembrane potentials, and conductance-voltage relationships induced by these dyes in neutral, phosphatidylethanolamine (PE)[1] and negatively charged, phosphatidylethanolamine/phosphatidylserine (PE/PS) bilayer membranes at various salt concentrations. The second paper (Krasne, 1980), which will be referred to as "paper II," examines the effects of these dyes on conductances mediated in these membranes by the ion carrier monactin and, by comparison with spectroscopic observations on cyanines in liposome suspensions, infers the degree to which the dyes modify the membrane's electrostatic potential (and fluidity) and to what extent these interactions are influenced by the dye structure, the surface charge density of the membrane, and the ionic strength of the aqueous phase.

Waggoner and his co-workers (Waggoner, 1976; Waggoner et al., 1977) have examined the instantaneous and steady-state currents produced by these dyes in glyceryl monoolein (GMO) and GMO-cholesterol bilayers in response to either single, square voltage pulses or pulse trains. Currents were found to increase with increasing hydrocarbon chain length and to decrease with increasing mole-percent cholesterol in the membrane. These authors then correlated the optical changes they observed for the same voltage pulses with the charge movements induced by the dyes, assuming that the membrane currents were carried by dissociated dye monomers because they found little variation in their observations for large variations in the types of salts (e.g., Na_2SO_4, KCl, $CaCl_2$, sodium 1,3,5-benzenetrisulfonate). (Note, however, that comparison of the data in Tables 2 and 3 of Waggoner et al. [1977], [or,

[1] *Abbreviations used in this paper:* G-H-K equation, Goldman-Hodgkin-Katz equation; GMO, glyceryl monoolein; PE, phosphatidylethanolamine; PS, phosphatidylserine.

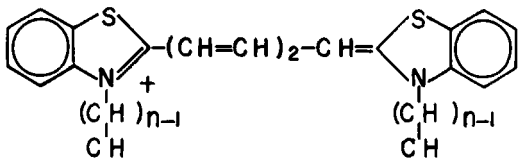

FIGURE 1 Structural formulas for the thiadicarbocyanine dyes used in the present studies. The value of n refers to the length of the hydrocarbon side chains attached to the tertiary amine. These dyes have a net, delocalized, positive charge and no fixed dipole moment.

for example, see columns 1 and 2 of Table I in the present paper] suggest that the ions present in the aqueous phase may affect these conductances.)

In the present paper we have examined effects of several of the same dyes, over a wide range of dye and salt concentrations, in phospholipid membranes which, because of their more positive dipole potentials than GMO bilayers, might be expected to exhibit different interactions with the dyes.

MATERIALS AND METHODS

Materials

Bacterial PE was obtained from Analabs (Analabs Inc., North Haven, Conn., 98% purity). Although this lipid is referred to here as "neutral", double-layer potential estimates, based upon the influence of varying ionic strength on the nonactin-NH_4^+ conductance (induced in planar, bilayer membranes; see McLaughlin et al., 1970), indicate a negative surface-charge density of approximately one charge per 3,000 $Å^2$. Bovine PS was obtained from Lipid Products (England), and *n*-decane was obtained from Aldrich (Aldrich Chemical Co., Inc., Milwaukee, Wisc., 99.9+% grade). All chemicals were used without further purification.

The cyanine dyes were a generous gift from Alan Waggoner (Amherst College). The dyes and ion carriers were kept as concentrated stock solutions in 99% ethanol and were stored in the refrigerator. Distilled water, subsequently passed through an organic scavenger and deionized to 18 $M\Omega\text{-}cm^2$ via a Millipore Q-2 water purification system (Millipore Corp., Bedford, Mass.), was used for preparation of solutions from analytical grade reagents. For all experiments, the solutions were unbuffered (i.e., they were maintained at pH 5.5 by atmospheric CO_2).

TABLE I
COMPARISON BETWEEN CONDUCTANCES INDUCED BY 1.5 μM $diSC_3(5)$ AND $diSC_5(5)$ IN GMO, PE, AND PE/PS BILAYERS

	GMO*, $\Omega^{-1}cm^{-2}$		PE‡, $\Omega^{-1}\,cm^{-2}$	PE/PS,‡ $\Omega^{-1}\,cm^{-2}$
	0.1 M KCl	0.08 M Na_2SO_4	0.1 M KCl	0.1 M KCl
$diSC_3(5)$	1.6×10^{-6}	1.83×10^{-6}	5.6×10^{-8}	2.8×10^{-7}
$diSC_5(5)$	2.03×10^{-5}	3.33×10^{-6}	1.1×10^{-7}	2×10^{-7}

*Calculated from Tables 2 and 3 of Waggoner et al., 1977. The data for 0.1 M KCl reflect the mean steady-state current for a series of 1-ms square waves varying between 0 and 75 mV divided by the mean voltage (0.0385 V). The data for 0.08 M Na_2SO_4 reflect the steady-state currents, reported in response to a 60-mV voltage step, divided by the voltage (i.e., 0.06 V).

‡These values were interpolated from the data of Figs. 2 and 3, in the present paper, for PE and PE/PS bilayers, respectively.

Methods

Membranes were formed on a Teflon partition separating two aqueous compartments containing 3.5-ml volumes each. The membrane-forming solution was composed of 25 mg of lipid per ml of decane. For PE/PS membranes, the ratio of PE to PS was 1:1. The black area of the membrane was monitored visually (using a stereomicroscope fitted with a graticule in one eyepiece); all measurements reported are for membranes which had been totally black for at least 15 min. Aliquots from stock solutions of dyes and carriers were added to the aqueous solutions. In the case of measurements for the highest concentration of $diSC_1(5)$, the aqueous solution contained 3% ethanol; for all other dyes, the final concentration of ethanol in the aqueous phase never exceeded 1%.

All experiments were performed at 23°C. Four Ag-AgCl electrodes were routinely used, two for passing current and two for monitoring voltage. A digital electrometer (model 616, Keithley Instruments, Inc., Cleveland, Ohio) was used to monitor the current and a differential electrometer (model 604, Keithley Instruments, Inc.) to monitor the transmembrane voltage. A waveform generator (model 144, Wavetek, San Diego, Calif.) supplied square wave pulses of ±10 mV (symmetrical about 0 mV, frequency 0.02 Hz) for monitoring the zero-current conductance, and the electrometer output was recorded via a Linear Data strip chart recorder (Linear Instruments Corp., Irvine, Calif.). For current-voltage measurements, ramps of voltage were applied (at rates of 1–25 mV/s) via the waveform generator and the currents and voltages across the membrane recorded on a Houston Instruments X-Y recorder (Houston Instruments Div., Bausch & Lomb, Inc., Austin, Tex.). Except when noted, the current-voltage relationships were independent of the rate of change of voltage over the range indicated.

RESULTS

As will be seen imminently, the permeability behaviors induced in bilayer membranes by these dyes are complicated and vary dramatically in going from the shortest- to the longest-chained dye. I shall first summarize my overall conclusions about the mechanisms by which these dyes induce membrane permeabilities as well as about their interactions with membranes, with each other, and with ions, and shall then present the data (in this as well as the following paper) on which these conclusions are based.

(*a*) The first conclusion is that dye-induced permeability varies with dye chain length along a continuum, with the shortest-chained dyes forming "voltage-gated" channels and the longest-chained dyes acting as anion carriers, forming 2:1 dye:anion species, as well as possibly being permeant species in their uncomplexed form. (*b*) Secondly (see paper II), the membrane/solution partition coefficient for the dye increases with increasing dye chain length whereas the electrostatic potentials produced by dye adsorption to the membrane go through a maximum with increasing chain length. (The origins of these electrostatic potentials are not specified here but could include "double-layer," dipole, and "boundary" potentials [McLaughlin, 1977].) (*c*) Finally, these dyes form spectroscopically identifiable aggregates in the membrane as well as in the aqueous phase. Aggregation generally increases with increasing chain length and with increasing salt concentration; however, there is a spectroscopically identifiable species observed for the shorter-chained dyes, but not the longer-chained dyes, which behaves like a form of dye aggregate and which increases with decreasing ionic strength.

Dye-Induced, Zero-Current Conductances

The steady-state, zero-current conductance behaviors mediated by the dyes in PE membranes are shown in Fig. 2 A–D for $diSC_1(5)$, $diSC_3(5)$, $diSC_5(5)$, and $diSC_8(5)$, respectively. The

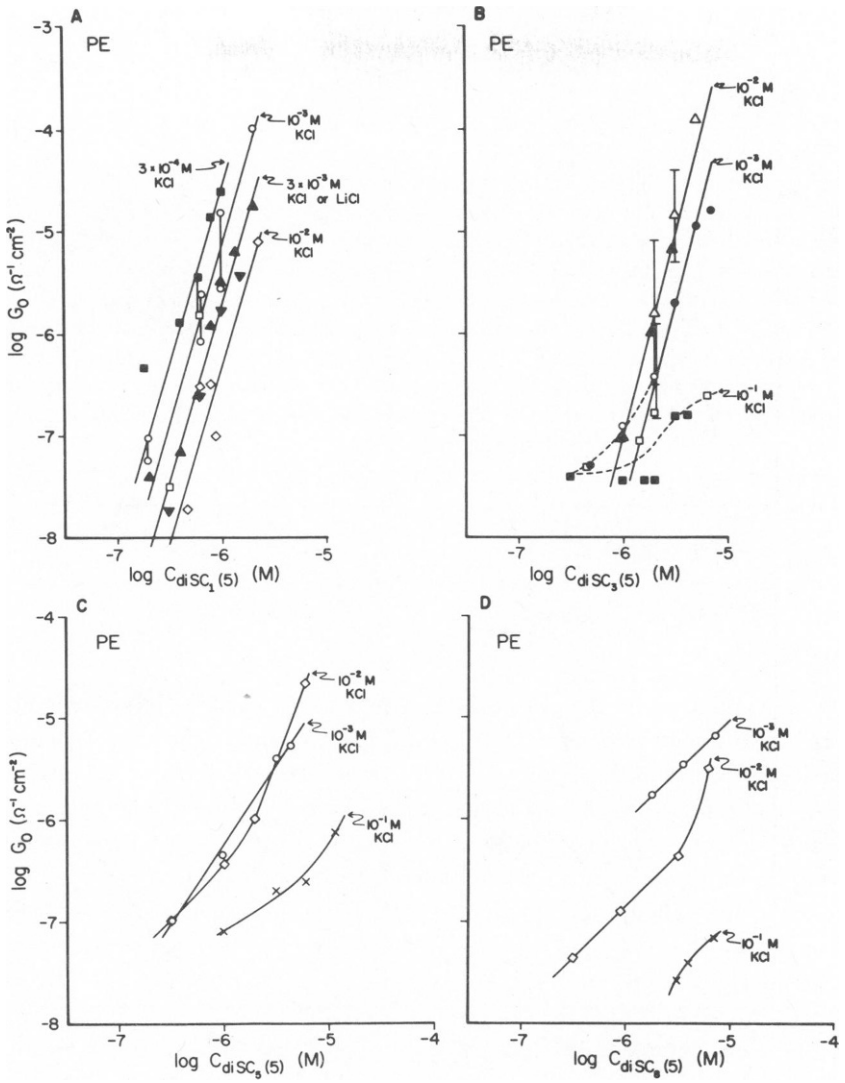

FIGURE 2 Steady-state, zero-current conductances induced in PE bilayers by symmetric $diSC_n(5)$. In all subfigures, the ordinate is the logarithm of the zero-current conductance and the abscissa is the logarithm of the concentration to which dye was added in the aqueous phase bathing each side of the membrane. All data values are corrected for the bare membrane conductance which ranged from 10^{-8} to 3×10^{-8} $\Omega^{-1}cm^{-2}$. (A) Data for $diSC_1(5)$. The open symbols indicate data from various membranes whereas any given type of closed symbol indicates values obtained from a single membrane. Correspondence between salt concentrations and symbols are as follows: 3×10^{-4} M KCl (■), 10^{-3} M KCl (○), 3×10^{-3} M KCl (▲), 3×10^{-3} M LiCl (▼), 10^{-2} M KCl (◇). The lines are drawn for slopes of 3.5. (B) Data for $diSC_3(5)$. A given type of closed symbol indicates measurements made on a single membrane. The bars represent ranges of data values when measurements were made for the same salt and dye concentrations in three or more bilayers. Correspondence between salt concentrations and symbols are as follows: 10^{-3} M KCl (●), 10^{-2} M KCl (△), 10^{-1} M KCl (□). The solid lines are drawn for slopes of 4. (C) Data for $diSC_5(5)$. Most data values for a given symbol represent measurements on a single membrane. The lines are drawn solely to try to connect the data points: 10^{-3} M KCl (○), 10^{-2} M KCl (◇), 10^{-1} M KCl (x). (D) Data for $diSC_8(5)$. Lines and symbols have the same meaning as in C.

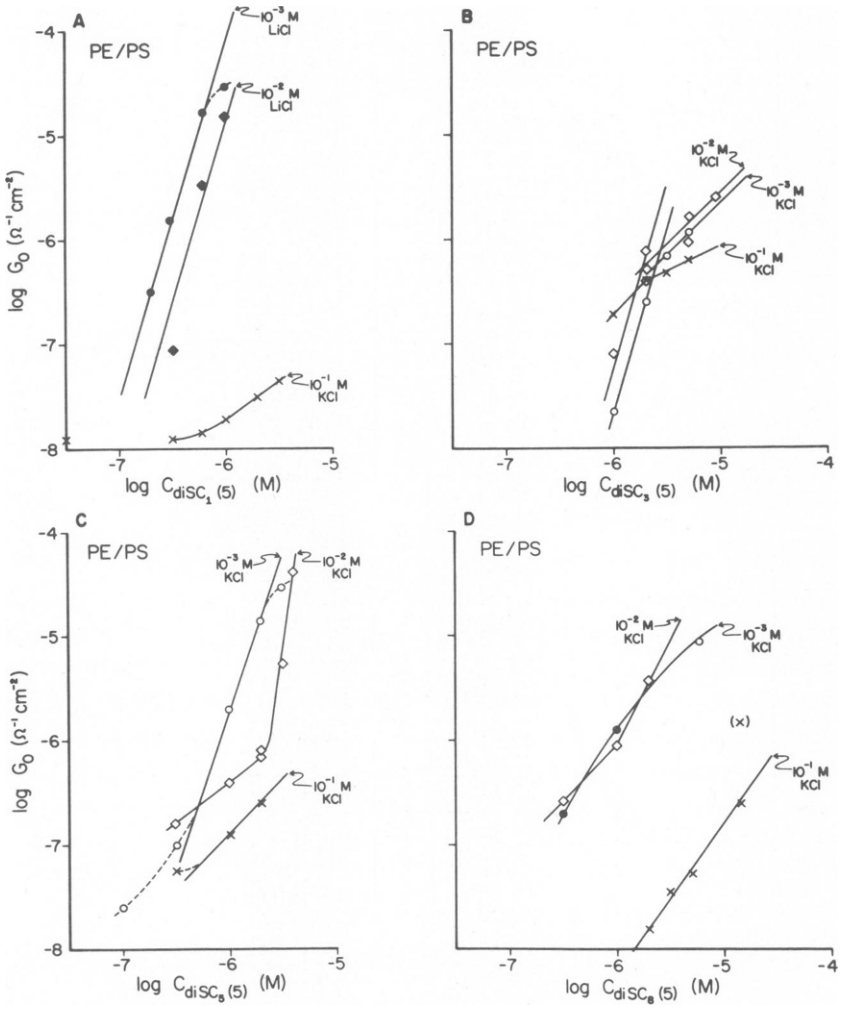

FIGURE 3 Steady-state, zero-current conductances induced in PE/PS bilayers by symmetric $diSC_n(5)$. The ordinate and abscissa are the same as for Fig. 1. (A) Data for $diSC_1(5)$. Filled symbols have the same meaning as in Fig. 1 A. Solid lines for 10^{-3} M and 10^{-2} M LiCl have slopes of 3.5. 10^{-3} M LiCl (●), 10^{-2} M LiCl (♦), 10^{-1} M LiCl (x). (B) Data for $diSC_3(5)$. All data points for a given salt concentration were obtained from a single membrane. Lines through the data for 10^{-3} M and 10^{-2} M KCl have slopes of 3.5 (steeper lines) and 1 (less steep lines). 10^{-3} M KCl (○), 10^{-2} M KCl (◇), 10^{-1} M KCl (x). (C) Data for $diSC_5(5)$. All data points for a given salt concentration were obtained from a single membrane except for the upper diamond for 2×10^{-6} M $diSC_5(5)$ in 10^{-2} M KCl. 10^{-3} M KCl (○), 10^{-2} M KCl (◇), 10^{-1} M KCl (x). (D) Data for $diSC_8(5)$. Data points for a given salt concentration were all obtained on a single membrane except for 10^{-3} M KCl for which the two filled symbols are for the same membrane. 10^{-3} M KCl (○), 10^{-2} M KCl (◇), 10^{-1} M KCl (x). The parenthesized x indicates the initial conductance value observed following the voltage step (this conductance decreasing with time to the indicated steady-state value).

analogous conductance behaviors in PE/PS bilayers are illustrated in Fig. 3 A–D. In all the experiments illustrated, the membrane was formed in a given salt solution and increasing amounts of dye were added to the same salt solution; virtually the same behaviors were observed for LiCl as for KCl solutions. (As is described more fully under conductance-voltage behaviors, dye-induced conductances may be assumed to be ohmic only for small (i.e. <25 mV) applied potentials. In the present paper, "zero-current" conductances refer to those measured for 10-mV applied potentials.)

Clearly each dye shows a different dependence of conductance on dye concentration. If one could describe the proportionality between the logarithms of conductance and dye concentration in Figs. 2 and 3 by the general relationship

$$\log G \propto N \cdot \log C_{dye} \tag{1}$$

then N would appear to decrease with increasing hydrocarbon chain length of the dye. One cannot draw a simple conclusion about the relative magnitudes of dye-induced conductances, however, because these depend upon the dye concentration, salt concentration, and the membrane composition in which the comparison is made.

Except at the higher ionic strengths (i.e. $\geq 10^{-1}$ M), and above 2×10^{-6} M $diSC_3(5)$ in PE/PS bilayers, the zero-current conductances induced by the two shorter-chain dyes appear to be steep functions of dye concentration, the value of N in Eq. 1 being 3.5 or 4 for PE and 3.5 for PE/PS bilayers. The major difference between the data for $diSC_1(5)$ and $diSC_3(5)$ is that the former dye appears to be about 5–10 times more effective than the latter in mediating membrane conductance. Most of the data for $diSC_1(5)$ and $diSC_3(5)$ come from steady-state measurements made on different membranes; however, the filled symbols in these zero-current conductance data represent measurements made on a single membrane for a given dye and a given salt concentration and clearly show the same trends as the other data.

In the case of the two longer-chained dyes, and the shorter-chained dyes at 0.1 M ionic strength, the conductances tend to be less steep functions of dye concentration as illustrated in Fig. 2 C and D for PE bilayers and Fig. 3 C and D for PE/PS bilayers. The slope of log conductance vs. log dye concentration varies with salt concentration and sometimes even with dye concentration for a given salt concentration (cf. data for 10^{-2} M salt in PE bilayers), and thus Eq. 1 does not readily apply in that N is not a constant. Despite this complication, one can see that a fit of Eq. 1 to these data would result in values of N which are 3 or less; it will be shown further on that after correcting for electrostatic potential effects, the value of N for much of the data tends towards 2.

To determine the mechanisms by which these dyes induce membrane conductances, it is useful to know the charge of the permeant species. If these dyes are either membrane-permeable ions themselves or act as carriers for an inorganic ion, then the sign of the charge on the current-carrying species can be ascertained by examining whether the conductance is enhanced or depressed in the negatively charged, PE/PS, bilayers as compared to the neutral, PE bilayers (McLaughlin et al., 1971; McLaughlin, 1975).

Comparison of dye-mediated conductances in neutral (PE) and negatively charged (PE/PS) membranes demonstrates that these conductances are either comparable in the two membranes or are higher in negatively charged membranes, especially at low dye concentrations. The generally higher conductances in PE/PS membranes suggest that, if the charge-

carrying species is the dye or a dye-ion complex, it is positively charged. For monactin-K^+, the conductance mediated in PE/PS bilayers (made from the same batch of lipids as in the above-mentioned experiment) is ~10 times higher than in PE at 0.01 M ionic strength. For dye-mediated conductances, the ratio of conductances in PE/PS to those in PE bilayers is usually less than that observed for monactin-K^+, presumably because of the alterations of electrostatic potentials by dye adsorption. However, for $diSC_1(5)$ the conductances produced in PE/PS bilayers at 0.01 M ionic strength are ~30 times larger than those observed for PE bilayers. This result suggests either that the charge-carrying species has a net charge of $\sim+1.5$ or that this dye molecule forms ion-conducting pores, each of which is composed of more than one dye molecule.

Considering the generally lower-order dependence of conductance on dye concentration for the longer-chained dyes (and $diSC_3(5)$ in 0.1 M salt concentrations) as well as their higher conductance-inducing capabilities in PE/PS than in PE bilayers, it is reasonable to postulate that these dyes may be acting either as lipid-soluble cations or as anion carriers. As shown below, the zero-current potentials and conductance-voltage behaviors are also consistent with the notion that the conducting species induced by $diSC_5(5)$ and $diSC_8(5)$, and by $diSC_3(5)$ at 0.1 M ionic strength, are monovalent cations. The conductances in Fig. 2 C, D, and 3 C, D are expected to have been altered by changes in the electrostatic potentials near the membrane surface produced by adsorption of the charged dye molecules, such changes being shown, in paper II, to exist. Presuming that this dye-induced electrostatic potential will have the same effect on all monovalent, cationic, permeant species, one can use the alterations by these dyes of monactin-K^+-mediated membrane conductances, reported in paper II, to correct for dye-induced electrostatic potentials (see, for example, McLaughlin, 1977).

The conductance data for $diSC_5(5)$ and $diSC_8(5)$, under conditions in which electrostatic-potential measurements could be made, and for $diSC_3(5)$ at 10^{-1} M ionic strength have been corrected for dye-induced electrostatic potentials reported in paper II and plotted as a function of the bulk aqueous dye concentrations in Fig. 4. The solid lines in this figure have been drawn for the value of N (in Eq. 1) = 2 and the broken line for N = 1.5. Clearly, for the range of salt and dye concentrations plotted in Fig. 4, it is quite reasonable to think that $diSC_3(5)$, $diSC_5(5)$, and $diSC_8(5)$ increase membrane conductances by mechanisms analogous to those which have been observed for a variety of weak acid uncouplers (LeBlanc, 1971; McLaughlin, 1972; Neumcke and Bamberg 1975; Smejtek et al., 1976; and Cohen et al., 1977), namely, by acting as 2:1 dye-anion complexes (by analogy to the 2:1 weak acid-hydrogen complexes) in the cases in which N = 2 (and possibly by having an additional conductance contributed by the uncomplexed, monomeric dye cation in the case in which N = 1.5).

Whereas the conductances increase with increasing dye concentration, they tend to decrease, or go through a maximum, with increasing salt concentration. In addition, at least for $diSC_1(5)$ and $diSC_3(5)$, the conductance at a high salt concentration (i.e. 0.1 M) fails to show the steep dependence of conductance on dye concentration seen at lower salt concentrations. In the experiments illustrated in Figs. 2 and 3, the data were obtained by adding successively larger aliquots of dye to a solution containing a given salt concentration. If, instead, the experiments were performed by adding successively larger aliquots of salt to a

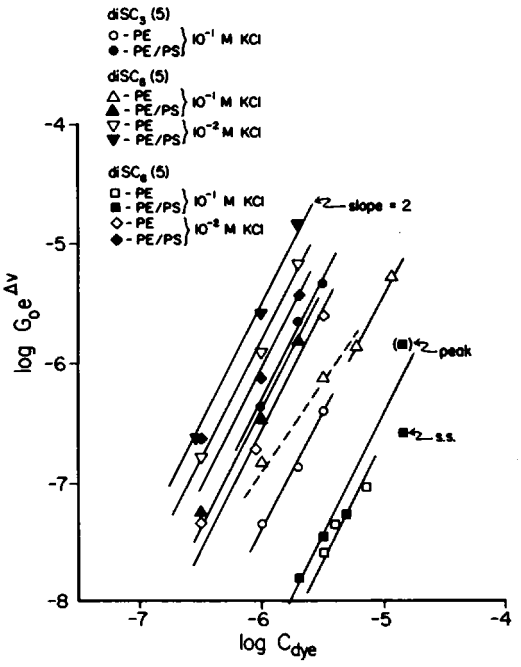

FIGURE 4 Steady-state, zero-current conductances corrected for dye-induced electrostatic potentials. The ordinate is the logarithm of the product of the observed zero-current conductances and the exponential of the dye-induced electrostatic potentials (in units of F/RT) calculated in paper II. The resulting data points indicate the relationship between zero-current conductance and dye concentration which should be observed if the dye did not alter the membrane's electrostatic potential. The solid lines have slopes of 2 and the broken line has a slope of 1.5. The symbols are defined in the figure.

solution containing a given concentration of dye (not illustrated), a fast increase in conductance, proportional to the first power of the salt concentration, was initially observed followed by a very slow, steady decline in conductance which, unfortunately, rarely reached a steady state before the membrane broke.

Whereas $diSC_1(5)$ produced significant conductances when added to both sides of PE bilayers, no conductance increase was observed when dye was added to only one side of the membrane. Additionally, asymmetrical concentrations of dye produced conductances equal to the geometric mean of the conductances observed when both aqueous solutions contained either the higher or the lower concentration of dye. In the cases of $diSC_3(5)$, $diSC_5(5)$, and $diSC_8(5)$, conductance increases were observed even when dye was present on only one side of PE membranes.

Despite the complicated dependences of dye-mediated conductances on dye and salt concentration and on lipid composition illustrated in Figs. 2 and 3, one can generally conclude that the conductance behaviors induced by $diSC_1(5)$ and $diSC_3(5)$ are qualitatively similar to each other whereas those induced by $diSC_5(5)$ and $diSC_8(5)$ tend to resemble each other but differ from those of the previous two dyes, especially in their less steep dependences of conductance on dye concentration. (Note that in PE/PS bilayers at high dye concentration

$diSC_3(5)$ appears to have a less steep dependence of conductance on dye concentration and thus behaves more like the longer-chained dyes. That this apparent "transition" in conductance behavior is meaningful will be further demonstrated below.)

Dye-Mediated, Zero-Current, Transmembrane Potentials

The data presented in Figs. 5–8 indicate that the zero-potential behaviors change in going from the shortest- to the longest-chained dyes and in combination with the zero-current conductance behaviors, further suggest that the shortest-chained dyes form ion-permeable pores whereas the longest-chained dyes increase membrane permeability by acting as lipid-soluble cations as well as by forming permeant, 2:1 dye-anion complexes.

The data in Figs. 5–8 represent transmembrane potentials recorded under three aqueous-solution conditions. In one condition, both aqueous compartments contain equal concentra-

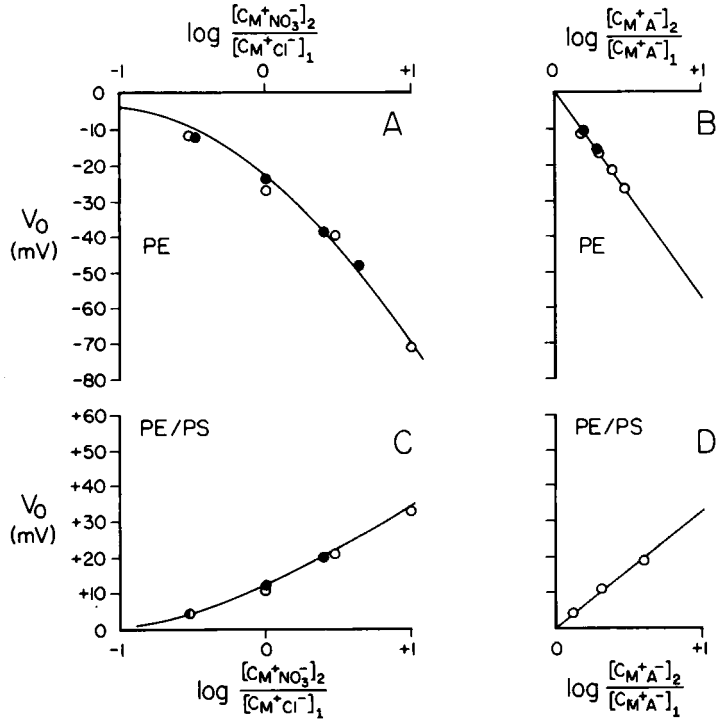

FIGURE 5 Zero-current potential behaviors observed for $diSC_1(5)$. For all zero-current potential measurements in Figs. 5–8, the reference electrode is on side 2 and all additions were made to the aqueous solution on side 2 of the membrane unless otherwise stated. (A) Mixed-ion, asymmetry potentials observed when KNO_3 was added to PE membranes bathed in symmetrical 10^{-3} M LiCl and 1.5×10^{-6} M $diSC_1(5)$ (○) or symmetrical 3×10^{-3} M KCl and 4×10^{-6} M $diSC_1(5)$ (●). The solid curve is that predicted by the G-H-K equation for ideal anion selectivity and $P_{NO_3^-}/P_{Cl^-} = 1.6$. (B) Salt-dilution potentials observed in PE membranes for gradients of KNO_3 in symmetrical, 4×10^{-6} M $diSC_1(5)$ (●) or gradients of LiCl in symmetrical, 2×10^{-6} M $diSC_1(5)$. The solid line has a slope of -58 mV/Δlog $C_{M^+A^-}$. (C) Mixed-ion asymmetry potentials observed when $LiNO_3$ is added to one side of PE/PS bilayers bathed in symmetrical, 10^{-2} M LiCl (●) or 10^{-3} M LiCl (○) and 10^{-6} M $diSC_1(5)$. The curve is drawn according to the G-H-K equation for $P_{Li^+}/P_{Cl^-} = 3.6$ and $P_{Cl^-}/P_{NO_3^-} = 1.7$. (D) Salt-dilution potentials observed in PE/PS bilayers for a gradient of LiCl in symmetrical, 3×10^{-7} M $diSC_1(5)$. The line is drawn according to the G-H-K equation for $P_{Li^+}/P_{Cl^-} = 3.6$.

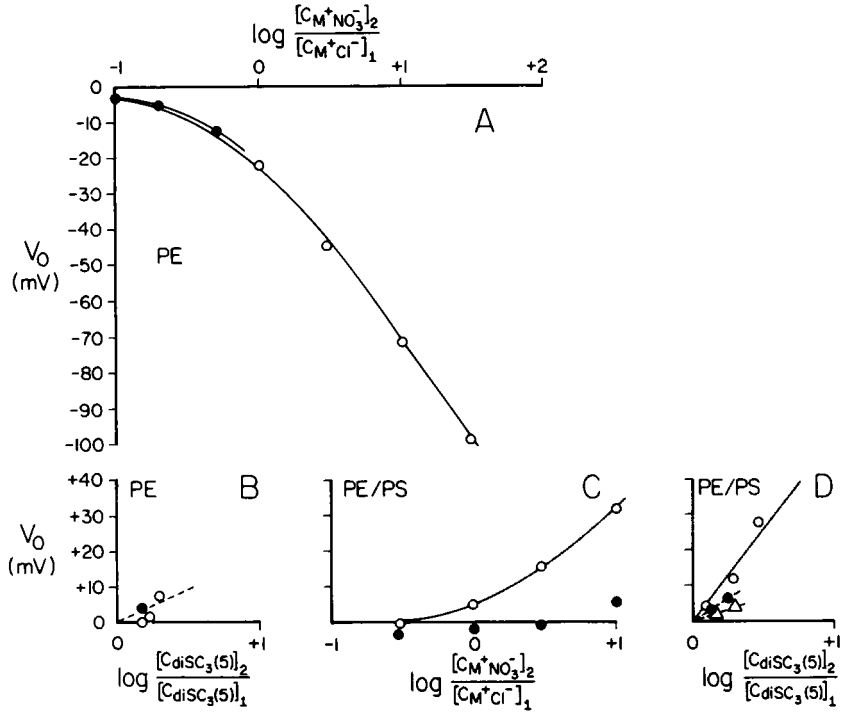

FIGURE 6 Zero-current potential behaviors observed for $diSC_3(5)$. (A) Mixed-ion, asymmetry potentials observed for additions of KNO_3 to PE bilayers bathed in symmetrical 10^{-3} M KCl and 4×10^{-6} M $diSC_3(5)$ (○) and 10^{-1} M KCl and 7×10^{-6} M $diSC_3(5)$ (●). The curves are drawn according to the G-H-K equation for ideal anion selectivity, with that through the open circles corresponding to $P_{NO_3^-}/P_{Cl^-} = 1.6$ and that through the closed circles corresponding to $P_{NO_3^-}/P_{Cl^-} = 1.3$. (B) Dye-dilution potentials observed for PE bilayers bathed in symmetrical 10^{-3} M KCl (●) or 10^{-2} M KCl (○). Dye additions were "see-sawed" across the membrane so that the left-most symbols represent higher total dye concentrations than the right-most ones. (C) Mixed-ion, asymmetry potentials observed upon adding KNO_3 to one side of PE/PS bilayers bathed in symmetrical 10^{-3} M KCl and either 2×10^{-6} M $diSC_3(5)$ (○) or 7×10^{-6} M $diSC_3(5)$ (●). The solid curve is drawn according to the G-H-K equation for $P_{Cl^-}/P_{K^+} = 3$ and $P_{K^+} \gg P_{NO_3^-}$. (D) Dye-dilution potentials observed for PE/PS bilayers when $diSC_3(5)$ is increased on one side of a membrane bathed in symmetrical 10^{-2} M KNO_3 ($+10^{-3}$ M KCl) and 2×10^{-6} M $diSC_3(5)$ (△), 5×10^{-6} M $diSC_3(5)$ (●) or 7×10^{-6} M $diSC_3(5)$ (○). The solid line has a slope of 58 mV/Δlog C_{dye}.

tions of KCl or LiCl, and aliquots of KNO_3 or $LiNO_3$, respectively, are added to one aqueous compartment and the resultant zero-current, mixed-ion potential measured. In plotting the data from these experiments, the abscissa is the logarithm of the ratio of NO_3^- to Cl^- salt concentrations (Figs. 5 A, C, 6 A, C, 7 A, C, and 8 A). In the second condition, a gradient of a single salt (either KCl or KNO_3) is made across the membrane and the resultant zero-current, salt-dilution potential measured. For these data, the abscissa is the ratio of salt concentrations either side of the membrane (Figs. 5 B, D, 7 B, and 8 B, C). In the above two conditions, the dye concentration is equal in both aqueous compartments. In the third condition, different concentrations of dye are added to either aqueous compartment (while maintaining symmetrical salt concentrations) and the resultant zero-current, dye-dilution potential measured (Figs. 6 B and D). In all of these figures, the ordinate gives the zero-current transmembrane potential corrected for any asymmetrical electrode potentials (e.g. the calculated Ag:AgCl

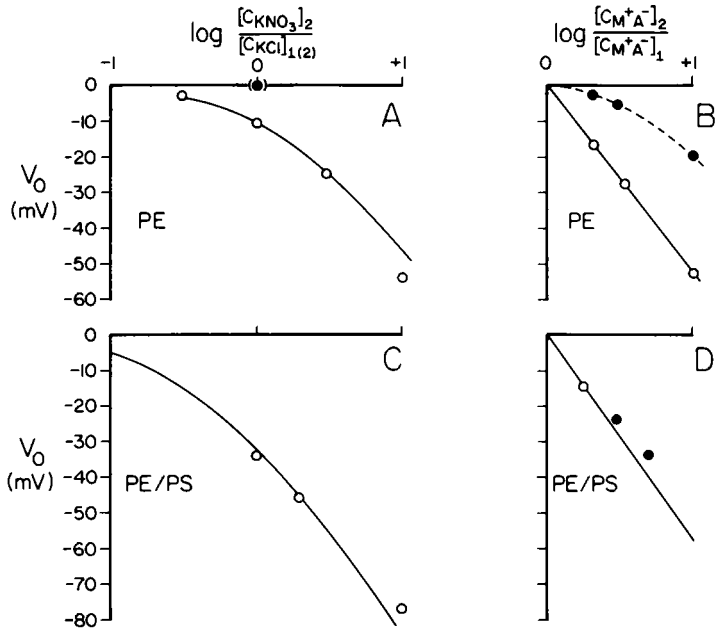

FIGURE 7 Zero-current potential behaviors observed for $diSC_5(5)$. (A) Mixed-ion asymmetry potentials observed in PE bilayers upon adding KNO_3 to one side of a membrane bathed in symmetrical 10^{-3} M KCl and 6×10^{-6} M $diSC_5(5)$ (○). The curve is drawn according to the G-H-K equation for ideal anion selectivity and the values of $P_{NO_3^-}/P_{Cl^-} = 0.54$. For the parenthesized, filled circles (and the corresponding parenthesized subscript on the abscissa designation), both solutions contain 6×10^{-6} M $diSC_5(5)$ and 2×10^{-2} M KNO_3, but side 2 contained 10^{-2} M KCl as well (whereas side 1 had 10 times less KCl than KNO_3). (Note that under the same conditions but when side 1 contains 10^{-2} M KNO_3 + 10^{-2} M KCl and side 2 contains 2×10^{-2} M KNO_3 + 10^{-2} M KCl, −17.5 mV are observed.) (B) Salt-dilution potentials observed for PE bilayers in the presence of symmetrical 6×10^{-6} M $diSC_5(5)$ and a gradient of KNO_3 (○) or KCl (●). The solid line is drawn with a slope of −58 mV/Δlog C_{salt}. (C) Mixed-ion asymmetry potentials observed upon adding KNO_3 to PE/PS bilayers bathed in symmetrical solutions of 10^{-3} M KCl and 6.75×10^{-6} M $diSC_5(5)$. The solid curve is drawn according to the G-H-K equation for ideal anion selectivity and $P_{NO_3^-}/P_{Cl^-} = 2.7$. (D) Salt-dilution potentials observed for PE/PS bilayers in the presence of 6.75×10^{-6} M $diSC_5(5)$ and a gradient of KNO_3 (○) or 4×10^{-6} M $diSC_5(5)$ and gradients of KCl (●). The solid line has a slope of −58 mV/Δlog C_{salt}.

electrode potential produced in asymmetrical Cl^- solutions was subtracted from the total potential), and the reference potential is that of the compartment to which the salt or dye addition was made (i.e., the reference electrode was on the side of higher salt or dye concentration).

For $diSC_1(5)$, zero-current, mixed-ion, and salt-dilution potentials were observed in both PE and PE/PS membranes (Fig. 5); however, no significant potentials were observed in the presence of asymmetrical dye concentrations (i.e., <5 mV for a 10-fold gradient of dye). In PE membranes (Fig. 5 A and B), $diSC_1(5)$ induces transmembrane potentials which behave as though the membrane were ideally selective for anions, the curve in Fig. 5 A having been drawn according to the Goldman-Hodgkin-Katz (G-H-K) equation (Goldman, 1943; Hodgkin and Katz, 1949), assuming that $P_{NO_3^-}/P_{Cl^-} = 1.6$ and that cations are impermeant. In PE/PS membranes, however, the transmembrane potentials were in the direction of greater

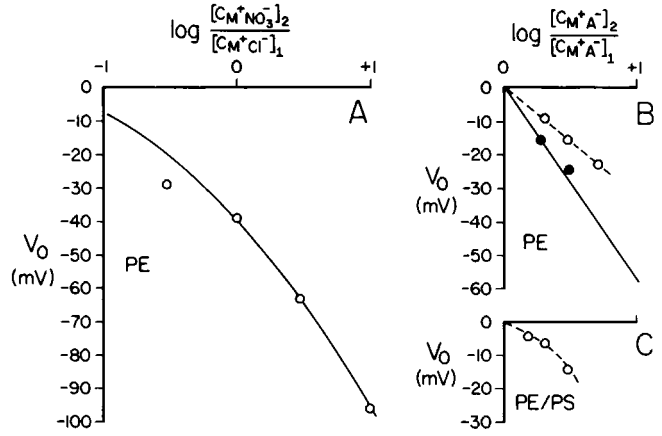

FIGURE 8 Zero-current potential behaviors observed for $diSC_8(5)$. (A) Mixed-ion asymmetry potentials observed upon adding KNO_3 to PE bilayers bathed in symmetrical 10^{-3} M KCl and 7×10^{-6} M $diSC_8(5)$. The solid curve is drawn according to the G-H-K equation for ideal anion selectivity and $P_{NO_3^-}/P_{Cl^-} = 4$. (B) Salt dilution potentials observed for PE bilayers bathed in symmetrical 6×10^{-6} M $diSC_8(5)$ and a gradient of KCl (○) or symmetrical 7×10^{-6} M $diSC_8(5)$ and a gradient of KNO_3 (●). The solid line has a slope of -58 mV/Δlog C_{salt}. (C) Salt-dilution potentials observed for a PE/PS bilayer bathed in symmetrical 1.5×10^{-5} M $diSC_8(5)$ and gradients of KCl.

cation than anion permeability. The curves in Fig. 5 C and D have been drawn according to the G-H-K equation assuming the values $P_{Li^+}/P_{Cl^-} = 3.6$, and $P_{Cl^-}/P_{NO_3^-} = 1.7$.

For $diSC_3(5)$, the zero-current potential behaviors induced in PE bilayers are virtually identical to those for $diSC_1(5)$, the curve in Fig. 6 A having been drawn according to the G-H-K equation assuming that $P_{NO_3^-}/P_{Cl^-} = 1.56$ and that cations are impermeant. In contrast to $diSC_1(5)$, however, zero-current potentials were seen in a gradient of $diSC_3(5)$ in PE bilayers at 10^{-2} M salt and low concentrations of dye, as illustrated in Fig. 6 B. In addition, $diSC_3(5)$ behaves quite differently from $diSC_1(5)$ in PE/PS bilayers, as illustrated in Fig. 6 C and D. The potentials observed upon adding aliquots of KNO_3 to one aqueous compartment, in the presence of symmetrical KCl and $diSC_3(5)$ solutions, are a function of the dye concentration. At 2×10^{-6} M $diSC_3(5)$ a fit of the G-H-K equation yields $P_{Cl^-}/P_{K^+} = 3$ and $P_K \gg P_{NO_3}$, whereas at 7×10^{-6} M dye, the membrane permeability appears to be virtually nonselective among cations and anions. Even more striking is the fact that steady-state, zero-current potentials are observed in the presence of a gradient of $diSC_3(5)$ (in symmetrical salt solutions) as is illustrated in Fig. 6 D; these potentials increase with both the gradient of dye and with the total dye concentration. Clearly, in PE/PS membranes at high dye concentrations, $diSC_3(5)$ is acting either as a lipid-soluble cation or as an anion carrier (the latter mechanism being consistent with the data of Figs. 6 C and D, as is discussed in the Discussion).

Finally, the zero-current potential behaviors induced by $diSC_5(5)$ and $diSC_8(5)$ are qualitatively similar to each other and behave in the following ways: (a) Potentials are observed in a gradient of salt which are in the direction of greater anion than cation permeability; however, these potentials are a function of total salt concentration and cannot be fit by the classical G-H-K equation. Attempts to fit the G-H-K equation to these data would

lead one to conclude that for salt-dilution potentials in a gradient of KCl, P_{Cl^-}/P_{K^+} generally increases with increasing salt gradient whereas for mixed-ion potentials observed upon adding KNO_3 to one side of a membrane bathed in symmetrical KCl and dye solutions, $P_{NO_3^-}/(P_{Cl^-} + P_{K^+})$ generally decreases with increasing salt gradient (although for $diSC_5(5)$ in PE bilayers it increases slightly). (b) In a gradient of dye, potentials are observed which tend to be larger at higher salt concentrations. They gradually decay with time for $diSC_5(5)$, and although usually <58 mV/decade, have a slope of ~80 mV per 10-fold gradient of dye in the case of $diSC_8(5)$ at 0.1 M salt concentration. (The potentials observed for gradients of $diSC_5(5)$ and $diSC_8(5)$, were quite variable and thus are not illustrated here. In several circumstances, however, steady-state potentials were observed which had slopes ≧58 mV/decade dye concentration. The transient potentials may be due to the asymmetrical production of electrostatic potentials.)

Dye-Induced Conductance-Voltage Behaviors

The voltage dependences of dye-induced conductances vary dramatically upon increasing the chain length of the dye, as seen in the "normalized" conductance-voltage behaviors illustrated in Figs. 9–12 for $diSC_1(5)$, $diSC_3(5)$, $diSC_5(5)$, and $diSC_8(5)$, respectively. In each of these figures, the ordinate is the "normalized" conductance, which is the conductance at a given

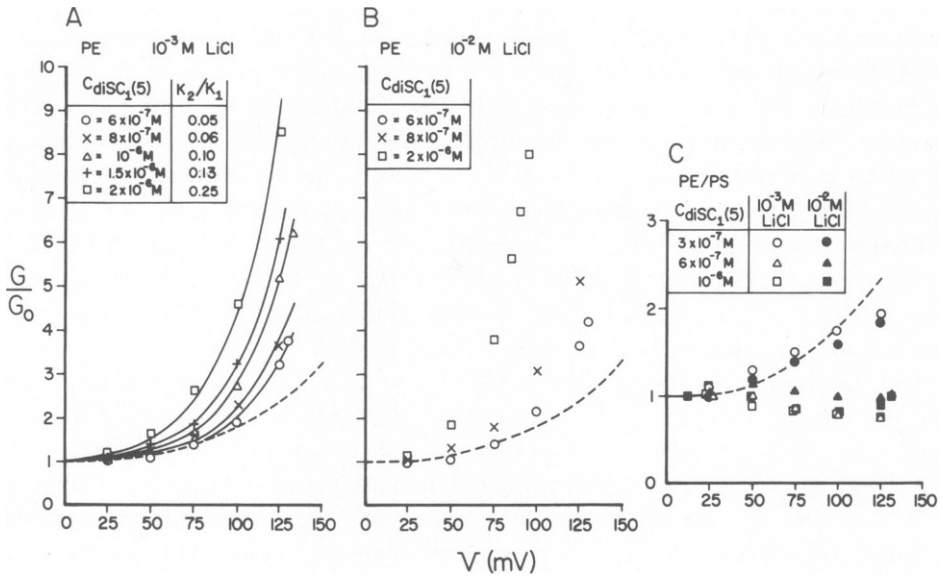

FIGURE 9 Normalized conductance-voltage behaviors induced by $diSC_1(5)$ into PE and PE/PS bilayers. In all subfigures of Figs. 9–12, the broken curve represents the normalized conductance-voltage behavior expected for a single Eyring barrier situated halfway through the membrane as discussed in the text. In addition, for all subfigures the ordinate is the conductance observed for a given transmembrane voltage divided by that observed in the limit of zero voltage, and the current-voltage relationships were obtained at sweep rates of 10 mV/s (Methods). The correspondence between the symbols and the solution conditions is indicated in each subfigure. (A) Data for 10^{-3} M LiCl and PE bilayers. The solid curves are drawn according to Eq. A9 in the Appendix for a value of $(\alpha_2 - \alpha_1)$ equal to 0.8 and for the values of K_2/K_1 indicated in this subfigure. See Appendix for details. (B) Data for 10^{-2} M LiCl and PE bilayers. (C) Data for 10^{-3} M and 10^{-2} M LiCl in PE/PS bilayers.

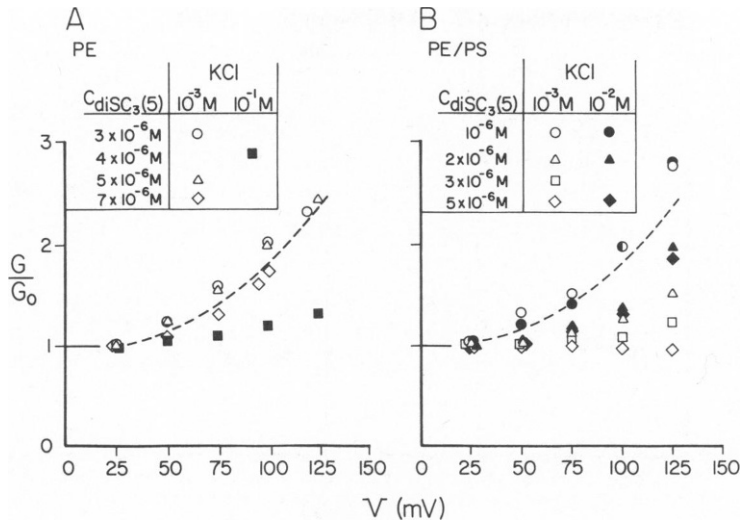

FIGURE 10 Normalized conductance-voltage behaviors induced by $diSC_3(5)$ in PE (A) and PE/PS (B) bilayers. Symbols are defined in each subfigure.

voltage divided by that in the limit of zero voltage, and the abscissa is the applied, transmembrane voltage. In addition, a broken curve appears in each figure and represents the normalized conductance-voltage behavior predicted by an Eyring rate theory approach for a single energy barrier situated halfway through the membrane (for example, Läuger and Neumcke, 1973); this broken curve represents the steepest voltage dependence of conductance which would be expected for a monovalent species permeating a symmetrical (about the midpoint) membrane either as a lipid-soluble ion, an ion-carrier complex, or via a nonvoltage-gated (symmetrical) channel.

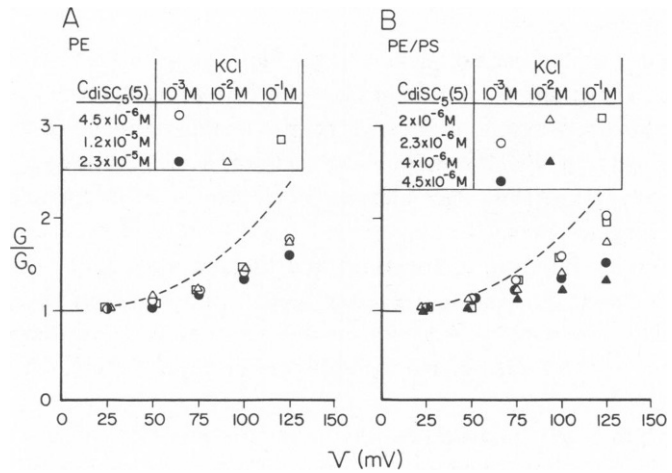

FIGURE 11 Normalized conductance-voltage behaviors induced by $diSC_5(5)$ in PE (A) and PE/PS (B) bilayers. Symbols are defined in each subfigure.

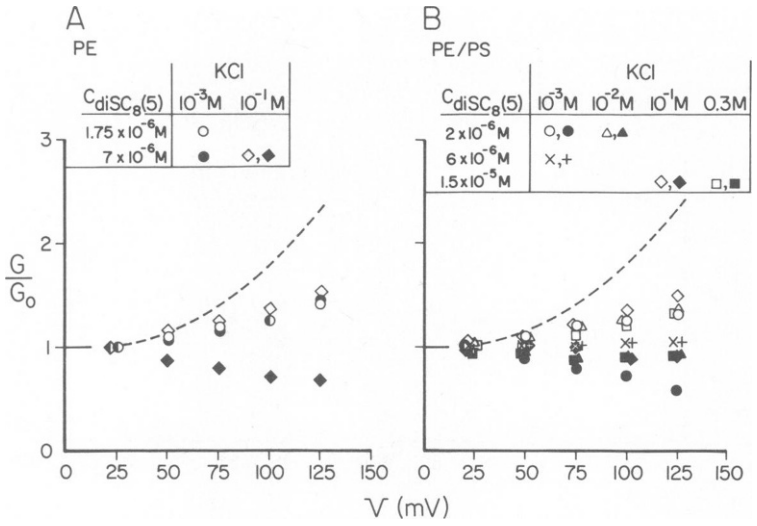

FIGURE 12 Normalized conductance-voltage behaviors induced by $diSC_8(5)$ in PE (A) and PE/PS (B) bilayers. Symbols are defined in each subfigure. When more than one symbol corresponds to a particular condition, the open symbols and the x correspond to the relationships observed for fast sweep rates of voltage (i.e. 25 mV/s) and the closed symbols and the + correspond to slow sweep rates of voltage (i.e., 2.5 mV/s).

The most striking features of the conductance-voltage behaviors illustrated in Figs. 9–12 are the following:

(*a*) The conductance behaviors induced by $diSC_1(5)$ in PE bilayers (Fig. 9 A) are much steeper functions of voltage than that predicted (cf. the broken curve in each figure) for a monovalent permeant species in the absence of "voltage-gating."

(*b*) Increasing the chain length of the dye decreases the voltage dependence of conductance, so that by $diSC_8(5)$ (Fig. 12), the conductance-voltage relationship is less steep than that given by the broken curve.

(*c*) The steepness of the conductance-voltage relationship increases with increasing dye concentration in PE membranes but decreases with increasing dye concentration in PE/PS membranes. (An apparent exception might appear to be the conductance-voltage relationship induced by $diSC_8(5)$ in PE/PS membranes. However, for this dye in this lipid the conductance shows a slow time dependence, and if one looks at the conductance-voltage relationship for high-frequency voltage ramps (i.e. 10–25 mV/s), one observes that the conductance generally increases with voltage and the steepness of the conductance-voltage relationship decreases with increasing dye concentration.) The dependence of the conductance-voltage relationship in PE bilayers on dye concentration is steepest for $diSC_1(5)$, becomes less steep with increasing chain length, and disappears (for high frequency voltage ramps) in $diSC_8(5)$.

(*d*) The steepness of the conductance-voltage relationship also varies with salt concentration. In PE membranes, the steepness of the conductance-voltage relationship increases with salt concentration for $diSC_1(5)$, and is approximately independent of salt concentration for $diSC_5(5)$ and (for high-frequency voltage ramps) $diSC_8(5)$. In PE/PS membranes the

steepness of the $diSC_3(5)$-induced conductance-voltage relationship increases with increasing salt concentration for intermediate and high dye concentrations but appears to be independent of salt concentration for low dye concentrations. As the side-chain length in increased, however, the conductance-voltage relationship becomes independent of salt concentration.

Considering the behaviors outlined above, one can view the conductance-voltage relationships induced by these dyes as a continuum in going from $diSC_1(5)$ to $diSC_8(5)$. However, detailed theoretical analysis of these behaviors based solely upon the present data will not be attempted here because of complicated effects of salt concentration, dye structure, and dye-induced electrostatic potentials on the partitioning of the dye between the aqueous and membrane phases as well as on the state of the dye in each phase, described in paper II.

In the Appendix a model is presented which demonstrates that the conductance-voltage behaviors observed for $diSC_1(5)$ in PE and PE/PS membranes could arise from the presence of a mixture of membrane-bound aggregates having, for example, different valences (e.g. dye-anion aggregates which are neutral and dye-anion aggregates which are positively charged) which form transmembrane, anion-permeable channels when aggregates from opposite sides of the membrane line up (as has been postulated for the polyenes nystatin and amphotericin B; Finkelstein and Holz, 1973).

DISCUSSION

The present paper has presented data on the effects of a series of carbocyanine dyes on the electrical properties of neutral and negatively charged phospholipid bilayer membranes in the presence of varied aqueous salt concentrations. The primary question behind these studies has been whether these dyes induce membrane permeabilities which are sufficiently large to alter the transmembrane potentials which they are presumably monitoring. The answer to this question depends to some extent upon the dye used, the aqueous salt concentration and surface charge density of the preparation being studied, the transmembrane potential itself, and the intrinsic membrane permeability. However, none of the four dyes studied produced significant alterations in membrane conductances at 0.1-M salt concentrations. These dye-induced conductances were always $<10^{-6}$ mhos/cm^2 at 10^{-5} M dye (and $\leq 10^{-7}$ mhos/cm^2 at 10^{-6} M dye, a concentration used more typically in biological experiments). For most biological membranes, conductances are typically 10^{-5} mhos/cm^2 or higher (see, for example, Cole, 1968). Cell membranes having lower conductance values would, of course, be subject to conductance perturbations induced by these dyes. The conductances induced by all of these dyes decreased with increasing salt concentration at potentials up to 125 mV and at dye concentrations up to $\sim 10^{-5}$ M (or 2×10^{-6} M in the case of $diSC_1(5)$). At lower salt concentrations, significant conductance changes were observed, especially with the two shorter-chained dyes, $diSC_1(5)$ and $diSC_3(5)$. It is unlikely that these dyes will induce extrinsic permeabilities of sufficient magnitude to affect cell and organelle membranes from most animals. However, in the case of animals, such as protozoa, whose "extracellular fluids" are typically lower than 10 mM ionic strength, the probability of these dyes perturbing the membrane potential is much more likely.

A second purpose of these studies was to investigate the mechanisms by which these dyes alter membrane permeabilities. This information bears not only on how the dyes alter membrane properties but also on how the dyes sense a transmembrane potential. For example,

it has been postulated by Waggoner and his colleagues (Waggoner, 1976; Waggoner et al., 1977) that the optical changes which occur in the dye spectrum shortly after applying a transmembrane potential result from a voltage-dependent redistribution of dye between the membrane and adjacent aqueous phases. These investigators have compared electrical currents induced by the dyes in glyceryl monooleate bilayers with the simultaneous changes in their optical signals in an effort to estimate how much dye is moving from the membrane to the aqueous phases (or vice versa) following a single voltage pulse. To make reasonable estimates, however, it is necessary to know whether the movement of one positive charge corresponds to the net movement of one dissociated dye molecule (as for the case in which the dye monomer acts as a hydrophobic ion), of a 2:1 dye-anion complex, or of an anion in the opposite direction (e.g. through a dye-induced pore). In the first case, the net movement of one positive charge corresponds to the movement of one dye molecule, in the second case to two dye molecules and in the third case to no dye molecules.

The results presented here suggest that in phospholipid membranes, cyanine dyes induce currents by a variety of mechanisms. For $diSC_1(5)$ the major mechanism appears to be the formation of (voltage-gated) anion-permeant pores. The major evidence for this mechanism comes from the following observations: (*a*) $diSC_1(5)$ produces a steep dependence of conductance on dye concentration. (*b*) Dye must be present on both sides of the membrane to observe a conductance increase. (*c*) The conductance shows a steep dependence on the transmembrane potential and this dependence is a function of the dye concentration, ion concentration, and membrane surface charge density. (*d*) The conductance-voltage relationship is rectifying when the dye concentration is different in the two aqueous compartments either side of the membrane (Appendix and Fig. 13). (*e*) Transmembrane potentials are not observed for asymmetrical dye concentrations but are observed for asymmetrical salt concentrations; these potentials imply an ideal ("Nernst") selectivity for anions over cations in PE membranes and an approximately 4:1 cation/anion selectivity in PE/PS membranes.

Whereas models can be formulated in which $diSC_1(5)$ acts as a carrier by forming a dye:anion complex that has a net charge >1 and thereby predict several of these observations, the lack of a conductance increase when dye is added to only one side of the membrane coupled with the observations of rectification in the conductance-voltage relationship but no zero-current potentials for asymmetrical dye concentrations argues compellingly that $diSC_1(5)$ forms ion-permeable pores. Whereas a definitive demonstration that this dye is a pore-former awaits noise or single-channel measurements, a model is presented in the Appendix which illustrates that all of the above observations are consistent with $diSC_1(5)$ forming aggregates which partition into (or at the surface of) the membrane and which form a transmembrane channel when two aggregates from either side of the membrane come into contact. The voltage dependence in this case arises because of the differential effect of voltage in driving the differently charged aggregates into or out of the plane in the membrane at which they come into contact with aggregates from the opposite side of the membrane.

The results presented are also consistent with the two longer-chained dyes acting as ion carriers, by forming lipid-soluble, 2:1 dye-anion complexes, and in some cases appearing to simultaneously permeate as a dye monomer. The main evidence for these mechanisms comes from the following observations: (*a*) The dye-mediated conductance increases as the second power, or in one case as the 1.5 power, of dye concentration when corrected for dye-induced

changes in the membrane's electrostatic potential (reported in paper II). (*b*) Steady-state conductance-voltage relationships are similar to those observed for other ion carriers and in some cases show the types of dependences on salt concentration, dye concentration, and time which have been observed previously for weak acids which form 2:1 complexes with hydrogen. (*c*) Zero-current potentials are observed for some asymmetrical concentrations of dye as well as for asymmetrical concentrations of salt. The dye-asymmetry potentials can be quite large transiently but in several cases tend towards lower levels with time. The salt-asymmetry potentials appear to depend upon the anion (i.e. NO_3^- vs. Cl^-) and upon the salt concentration; typically dilution potentials deviate from those expected from the Nernst equation with decreasing salt concentration whereas mixed-ion asymmetry potentials tend to deviate somewhat less from the expectations of the G-H-K equation.

The most compelling reasons to think that these two dyes are acting as carriers (and to some extent hydrophobic cations) come from the stoichiometries of the conductance vs. dye concentration relationship and the observations of transmembrane potentials for asymmetrical dye concentrations. For the weak acid uncouplers which form 2:1 complexes, transmembrane potentials for asymmetrical uncoupler have been reported previously only under the condition that hydrogen was not adequately buffered up to the membrane surface (Foster and McLaughlin, 1974) in which case $\Delta V/\Delta pH$ was <58 mV for both a dye gradient and a hydrogen gradient. For this case raising the buffering capacity of the aqueous solution gave rise to "Nernst potentials" in a gradient of hydrogen and no potential in a gradient of weak acid. The potential in a gradient of uncoupler arose in the case of lowered buffering because the free H^+ concentration at the interface, and thus the concentration of 2:1 complexes, could be altered by complexation with the uncoupler. In the present case of the dyes, the postulated 2:1 complex would be formed with an anion whose concentration is several orders of magnitude higher than that of the dye so it is unlikely that a difference in the total dye concentration on either side of the membrane could produce a significant difference in the concentration of the uncomplexed anion. By contrast, it can be shown that steady-state potentials are expected to be observed for differences in the total dye or salt concentrations on either side of the membrane when one assumes that the 1:1 complex diffuses slowly enough in the membrane (relative to the reactions at the interface and diffusion in the unstirred layers) that a gradient of this complex exists within the membrane. Furthermore, the deviations from the predictions of the Nernst and G-H-K equations observed for salt-dilution and mixed-ion asymmetry potentials, respectively, can be rationalized by the same assumption. (Such results are obtained when one assumes that the 2:1 dye-anion species is much more permeant in the membrane than any other species; however presentation of a detailed derivation of this result is beyond the scope of the present paper.)

The results observed for $diSC_3(5)$ suggest that it alters membrane conductances by acting as a pore-former, by acting as a lipid-soluble cation, and by forming 2:1 dye-anion complexes, depending upon the surface charge of the lipid and the dye and ion concentrations. More specifically, at low salt concentrations in PE bilayers the conductance shows a steep dependence on dye concentration, the conductance-voltage relationships are somewhat "steeper-than-Eyring," zero-current potentials imply ideal anion selectivity in a gradient of salt, and when the dye concentration is asymmetrical, zero-current potentials are observed only at very low dye concentrations (in which region a "carrier" or "hydrophobic cation"

mechanism may predominate over a "pore-former" mechanism). In PE/PS bilayers, $diSC_3(5)$ appears to act predominantly as a pore-former for dye concentrations of 2×10^{-6} M and lower based upon a steep dependence of conductance on dye concentration, a slightly steeper-than-Eyring conductance-voltage relationship and zero-current potentials in salt gradients suggesting greater cation than anion permeability. At higher dye concentrations, $diSC_3(5)$ appears to act as a hydrophobic cation (or possibly forms lipid-soluble, 2:1 dye-anion complexes). The main evidence for this mechanism is the development of sizable, steady-state, zero-current potentials for asymmetrical dye concentrations; at the highest dye concentrations these potentials approach those predicted by the Nernst equation. In addition, a marked decrease in the dependence of conductance on dye concentration and in the steepness of the conductance-voltage relationship are observed along with the disappearance of zero-current potentials for a gradient of salt concentration across the membrane. At 10^{-1} M salt concentration in both PE and PE/PS bilayers, $diSC_3(5)$ appears to form membrane-permeable, 2:1 dye-anion complexes as judged from a second-power dependence of conductance on dye concentration (after correction for dye-induced electrostatic-potential changes; see paper II), higher conductances in negatively charged than in neutral bilayers, zero-current potentials for asymmetrical dye concentrations, mixed-ion, zero-current potentials in asymmetrical salt solutions suggesting an ideal anion selectivity, and conductance-voltage relationships which are less-steep-than-Eyring.

It is of some interest to compare the results of the present studies with those obtained by Waggoner et al. (1977) using GMO/decane bilayers and 0.1 M KCl or 0.08 M Na_2SO_4 solutions for the series of cyanine dyes $diSC_n(5)$, where $n = 2, 3, 4$, or 5. From the data in their Tables 2 and 3 and their statement that the current-voltage curves were linear up to ~60 mV, I have estimated the conductances in GMO membranes and compared them in Table I to those observed here for $diSC_3(5)$ and $diSC_5(5)$. Clearly the conductances observed for the present PE and PE/PS bilayers are much lower than those observed for GMO bilayers. This observation is, in fact, consistent with the notion that the permeant species bears a net positive charge because the dipole potential in GMO bilayers is ~160 mV more negative than that of PE bilayers (Szabo et al., 1973) and, based upon the relative conductance observed for monactin-K^+ in the present work, is ~114 mV more negative than PE/PS bilayers at 0.1 M ionic strength. (Because the electrostatic potential difference observed inside GMO bilayers, relative to the aqueous phase, is independent of the ionic strength of the solution [as a result of its dipolar origin] whereas that of PE/PS increases with decreasing ionic strength [because of the net surface charge], this difference would be less at lower ionic strength.) Indeed, Waggoner et al. (1977) demonstrated that the dye-induced conductances decreased when the membrane's dipole potential was made more positive with cholesterol. In interpreting their optical data, these authors assumed that these dyes act as hydrophobic, monomeric, cations in increasing membrane conductance whereas the results in the present work suggest that in PE and PE/PS bilayers at 10^{-1} M KCl these dyes act as dimers (along with one anion) in increasing membrane conductance. Thus in these phospholipid bilayers at 0.1 M ionic strength, the net movement of one positive charge across the membrane would correspond to the net movement of a dimer rather than of a monomer of dye.

Received for publication 29 May 1979 and in revised form 24 January 1980.

APPENDIX

The purpose of this Appendix is to describe certain physical models which could give rise to the types of conductance and zero-current potential behaviors observed for $diSC_1(5)$. The specific behaviors which must be accounted for are the following:

(*a*) A steep dependence of zero-current conductance on dye concentration. (*b*) Higher zero-current conductances in negatively charged than neutral membranes. (*c*) Zero-current potentials which behave for PE as though membranes were ideally selective for anions, whereas for PE/PS as though cations were more permeant than anions. (*d*) A steep dependence in neutral membranes of "normalized" conductance on voltage which becomes steeper with increasing dye and/or ion concentration (at least up to 10^{-2} M salt). (*e*) A less steep dependence of (normalized) conductance on voltage in negatively charged membranes which decreases with increasing dye (this decrease being less at higher salt concentrations). (*f*) A lack of conductance increase (even at large potentials) when dye is present on only one side of the membrane.

Point *f* makes it seem more likely that this dye is acting as a pore-former than either as a lipid-soluble ion or an ion carrier. Therefore, we shall first consider pore-former models. The easiest model to conceive of intuitively which is consistent with the above observations is the one in which a pore is formed when aggregates of dye molecules from each side of the membrane meet (similar to that postulated for the polyene antibiotics; Finkelstein and Holz, 1973) and in which the steep dependence of conductance on voltage is derived from an effect of voltage in increasing the probability of aggregates meeting. For example, the aggregates might sit near the surface of the membrane and transmembrane-pore formation might require that they be pushed more towards the membrane interior. If only one type of aggregate existed and the effect of voltage were to push it into (or out of) the membrane, then the probability of forming a transmembrane pore would be independent of voltage, since the same fraction of "half-pores" should be pushed out of one side of the membrane as are pushed into the other side (and the density of transmembrane pores should be proportional to the product of the densities of "half-pores" either side of the membrane). By contrast, two or more types of aggregates might exist, each with a different dependence on voltage for its "repositioning" in the membrane (e.g., because each one has a different net charge or because the minimum energy position for each one is different so that they have to be driven different distances into the membrane before meeting up with a contralateral aggregate). In the case of two types of aggregates, the conductance would be given by,

$$G = gN^{Ch} \tag{A1}$$

and

$$N^{Ch} = p(SK_1'e^{\alpha_1\Delta\phi} + SK_2'e^{\alpha_2\Delta\phi})(SK_1''e^{-\alpha_1\Delta\phi} + SK_2''e^{-\alpha_2\Delta\phi}). \tag{A2}$$

N^{Ch} is the density of transmembrane pores, p is a (voltage-independent) proportionality constant (with units of area), g is the conductance of a single pore (which is assumed here to be the same for both types of pores), and α_1 and α_2 are the charge times the fraction of the transmembrane voltage which is traversed before meeting a contralateral aggregate, for aggregates 1 and 2, respectively. The superscripts (′) and (″) designate each side of the membrane, K_1 and K_2 are the densities of "sites" (normalized to be dimensionless) containing aggregates 1 and 2, respectively, at zero transmembrane potential, and S is the density of available "sites" into which an aggregate can move, a site being defined as a position within the membrane at which an aggregate (upon meeting a contralateral aggregate) will form a transmembrane pore.

The conservation equation for the total density of membrane sites, S^{TOT}, on a given side of the membrane is

$$S^{TOT} = S + K_1^* + K_2^*, \tag{A3}$$

where K_1^* and K_2^* are the densities of occupied sites, which equal the densities of aggregates already occupying sites on that side of the membrane (i.e. in a position from which they are able to form a

transmembrane pore) and are given by,

$$K_1^* = K_1 e^{\alpha_1 \Delta\phi} S \tag{A4}$$

and

$$K_2^* = K_2 e^{\alpha_2 \Delta\phi} S. \tag{A5}$$

Thus,

$$S = \frac{S^{TOT}}{1 + K_1 e^{\alpha_1 \Delta\phi} + K_2 e^{\alpha_2 \Delta\phi}}, \tag{A6}$$

for a given side of the membrane.

Combining Eqs. A2, A6, and A1 (and assuming S^{TOT} is the same either side of the membrane) gives the conductance equation

$$G = \frac{pg(S^{TOT})^2(K_1' + K_2' e^{(\alpha_2 - \alpha_1)\Delta\phi})(K_1'' + K_2'' e^{(\alpha_1 - \alpha_2)\Delta\phi})}{(1 + K_1' + K_2' e^{(\alpha_2 - \alpha_1)\Delta\phi})(1 + K_1'' + K_2'' e^{(\alpha_1 - \alpha_2)\Delta\phi})}. \tag{A7}$$

Assuming, for the sake of tradition, that the voltage dependence of the single-channel conductance, g, is negligible, the "normalized" conductance-voltage relationship is then given by

$$\frac{G}{G_0} = \frac{\left(1 + \frac{K_2'}{K_1'} e^{(\alpha_2 - \alpha_1)\Delta\phi}\right)\left(1 + \frac{K_2''}{K_1''} e^{(\alpha_1 - \alpha_2)\Delta\phi}\right)(1 + K_1' + K_2')(1 + K_1'' + K_2'')}{\left(1 + \frac{K_2'}{K_1'}\right)\left(1 + \frac{K_2''}{K_1''}\right)\left(1 + K_1' e^{\alpha_1 \Delta\phi} + K_2' e^{\alpha_2 \Delta\phi}\right)\left(1 + K_1'' e^{-\alpha_1 \Delta\phi} + K_2'' e^{-\alpha_2 \Delta\phi}\right)}. \tag{A8}$$

In the limit in which the density of available sites is approximately equal to the total density of sites, the right two parenthesized terms in the numerator and the denominator will equal 1 and the normalized conductance will reduce to

$$\frac{G}{G_0} = \frac{\left(1 + \frac{K_2'}{K_1'} e^{(\alpha_2 - \alpha_1)\Delta\phi}\right)\left(1 + \frac{K_2''}{K_1''} e^{(\alpha_1 - \alpha_2)\Delta\phi}\right)}{\left(1 + \frac{K_2'}{K_1'}\right)\left(1 + \frac{K_2''}{K_1''}\right)}. \tag{A9}$$

The data of Fig. 9 A have been fit with Eq. A9 for the case in which the solutions on either side of the membrane are identical, so that $(K_2'/K_1') = (K_2''/K_1'') = (K_2/K_1)$. For each individual dye-concentration curve, there was a range of values for $(\alpha_2 - \alpha_1)$ between 0.7 and 0.9 which would yield acceptable fits; however, simply allowing both $(\alpha_2 - \alpha_1)$ and K_2/K_1 to vary precluded the observation of any trends in either variable as a function of dye concentration. I therefore tried to find values of these parameters which, upon fitting the data, yielded monotonic trends in either K_2/K_1 or $(\alpha_2 - \alpha_1)$ or both. Upon imposing this constraint it was found that as good a set of curve-fits could be obtained by simply holding $(\alpha_2 - \alpha_1)$ constant at 0.8 and letting K_2/K_1 vary as for any other approach. This procedure yielded the set of curves illustrated by the solid lines in Fig. 9 A, the values of K_2/K_1 for each curve being listed in the inset of this figure. Interestingly, the ratio K_2/K_1 seems to increase approximately proportionally to the dye concentration. Since each of these K's should be proportional to the concentration of the particular aggregate, this observation suggests that (assuming the validity of this physical picture) the aggregate with the steeper voltage dependence is composed of one more dye molecule than that with the less steep voltage dependence. (That is, $K_1 = k_1(C_{dye})^m$, $K_2 = k_2(C_{dye})^n$, and $n - m = 1$. Note that this interpretation assumes that a sufficiently small fraction of the total dye is in the form of aggregates that

the dye monomer concentration in the membrane is not significantly reduced by aggregate formation.) In the case of the data at 10^{-2} M LiCl in Fig. 9 B, a higher value of $(\alpha_2 - \alpha_1)$ is necessary to procure a good fit. Indeed, for the curve at 2×10^{-6} M $diSC_1(5)$, the best fit was obtained by setting $(\alpha_2 - \alpha_1) = 1$ (for which $K_2/K_1 = 0.25$), and the curve could not be fit at all for values of $(\alpha_2 - \alpha_1) \leq 0.9$.

In line with the present model, the saturations in the normalized conductance-voltage behaviors seen for low dye concentrations and the lack of dependence of conductance on voltage (or slightly inverse dependence) at higher dye concentrations observed for PE/PS bilayers and illustrated in Fig. 9 C would arise from the effect of increased dye aggregates in the membrane depleting the density of unoccupied sites. Thus, in the limit in which $K_1 + K_2 \gg 1$,

$$\lim_{(K_1 + K_2) \to \infty} (G/G_0) = 1 \tag{A10}$$

and the normalized conductance becomes independent of voltage. Similarly, if the voltage is sufficiently large that $[K_1 \exp(\alpha_1 \Delta\phi) + K_2 \exp(\alpha_2 \Delta\phi)] \gg 1$, the normalized conductance-voltage relationship will saturate. These behaviors are indeed observed in Fig. 9 C. (The slightly inverse dependence of conductance on voltage observed in this figure for high dye concentration could arise, in terms of this model, from a small voltage dependence of the single-channel conductance.)

An alternative, and somewhat more appealing model, for the behaviors listed above would be similar to the present one except that the voltage dependence of conductance would arise from an effect of thinning the membrane (White, 1970) and thereby bring aggregates from opposite sides of the membrane in contact (rather than driving dye into and out of the membrane). In this model, because increased voltage brings dye from both sides of the membrane closer to the membrane's center, the conductance equation would have the form (for negligible saturation of "sites")

$$G\alpha[K'e^{f(v)}]\,[K''e^{(v)}] \tag{A11}$$

where K' and K'' are functions of dye concentration and $f(v)$ is proportional to the voltage dependence of membrane thinness (i.e. 1/thickness) which, according to White (1970), is dependent on the square of voltage.

A major difference between Eqs. A11 and A7 or A9 is that the latter two equations predict rectification of the conductance-voltage relationship in the presence of asymmetrical dye concentrations either side of the membrane whereas the former does not. I therefore examined the conductance-voltage behavior observed in the presence of asymmetrical dye and the results are presented as triangles in Fig. 13. The filled triangles represent the normalized conductances observed when the voltage is positive on the side of the membrane containing 10^{-6} M $diSC_1(5)$ and the open triangles represent the normalized conductances when the voltage on the side containing 6×10^{-7} M $diSC_1(5)$ is positive. For comparison, the closed and open circles represent the normalized conductance-voltage relationships observed (cf. Fig. 9 A) in the presence of symmetrical solutions containing 6×10^{-7} M and 10^{-6} M $diSC_1(5)$, respectively. First of all, the conductance-voltage behavior shows clear rectification in the presence of asymmetrical dye concentrations, ruling out the model in which pore formation is the result of voltage-induced membrane thinning. More specifically, however, for the first model to appear valid, it should be possible to fit the asymmetrical conductance-voltage data using the parameters deduced for the two cases of symmetrical dye concentrations illustrated by the circles in Fig. 13 (or by the circles and triangles in Fig. 9 A). For symmetrical 6×10^{-7} M $diSC_1(5)$ it was found that $K_2/K_1 = 0.05$ whereas for 10^{-6} M, $K_2/K_1 = 0.10$; for both cases $(\alpha_2 - \alpha_1) = 0.8$. The solid curves in Fig. 13 represent the normalized conductance-voltage relationships predicted (for positive and negative voltages) from Eq. A9 for $(K_2'/K_1') = 0.1$, $(K_2''/K_1'') = 0.05$ and $(\alpha_2 - \alpha_1) = 0.8$. They fit the data reasonably well.

It is worth noting that the data of Fig. 9 A (and B) can be fit by almost any theory which predicts exponential-like dependences of conductance on voltage, including, for example, a "Wein dissociation field effect" such as that discussed for picrate by Läuger and Neumcke (1973). In the case of a Wien effect, however, it is harder to predict why the zero-current conductance would have such a steep dependence on dye concentration, why dye would be ineffective when added to only one side of the

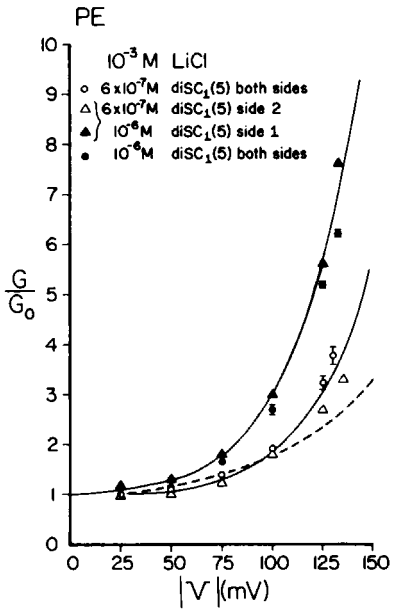

FIGURE 13 Rectification in the conductance-voltage behaviors induced by asymmetrical concentrations of $diSC_1(5)$. The ordinate is the normalized conductance observed for PE bilayers at the absolute value of voltage indicated by the abscissa. The circles are the mean data values ($n = 3$) for symmetrical concentrations of either 6×10^{-7} M $diSC_1(5)$ (○) or 10^{-6} M $diSC_1(5)$ (●), the bars representing 1 SD. The triangles are the data values when the aqueous phase on one side of the membrane contained 6×10^{-7} M $diSC_1(5)$ and the other side contained 10^{-6} M $diSC_1(5)$. For the filled triangles, the voltage on the side of the membrane with the higher dye concentration was positive whereas for the open triangles, the side with the lower dye concentration was positive. The solid curves are drawn according to Eq. A9 for the values $(\alpha_2 - \alpha_1) = 0.8$ and for $(K_2'/K_1') = 0.1$ and $(K_2''/K_1'') = 0.05$ as deduced for symmetrical concentrations of 10^{-6} M and 6×10^{-7} M dye, respectively (see text), from the data in Fig. 9 A. The salt concentration is 10^{-3} M LiCl, and the broken curve is the Eyring single-barrier prediction.

membrane and why such steep rectification in the conductance-voltage behaviors should be observed in the presence of asymmetrical dye concentrations.

REFERENCES

COHEN, F., M. EISENBERG, and S. MCLAUGHLIN. 1977. The kinetic mechanism of action of an uncoupler of oxidative phosphorylation. *J Membr. Biol.* **37**:361–396.

COHEN, L., and B. SALZBERG. 1978. Optical measurement of membrane potential. *Rev. Physiol. Biochem. Pharmacol.* **83**:35–88.

COHEN, L., B. SALZBERG, H. DAVILA, W. ROSS, D. LANDOWNE, A. WAGGONER, and C. WANG. 1974. Changes in axon fluorescence during activity: membrane probes of membrane potential. *J. Membr. Biol.* **19**:1–38.

COLE, L.S. 1968. Membranes, Ions and Impulses. University of California Press, Berkeley. 60.

FINKELSTEIN, A., and R. HOLZ. 1973. Aqueous pores created in thin lipid membranes by the polyene antibiotics nystatin and amphotericin B. *In* Membranes—A Series of Advances. G. Eisenman, editor. Marcel Dekker, Inc., New York. **2**:377.

FOSTER, M., and S. MCLAUGHLIN. 1974. Complexes between uncouplers of oxidative phosphorylation. *J Membr. Biol.* **17**:155–180.

GOLDMAN, D.E. 1943. Potential, impedance, and rectification in membranes. *J. Gen. Physiol.* **27**:37–60.

HAYNES, D.H., and P. SIMKOWITZ. 1977. 1-Anilino-8-naphthalenesulfonate: a fluorescent probe of ion and ionophore transport kinetics and trans-membrane asymmetry. *J. Membr. Biol.* **33**:63–108.

HODGKIN, A.L., and B. KATZ. 1949. The effect of sodium ions on the electrical activity of the giant axon of the squid. *J. Physiol. (Lond.).* **108**:37–77.

KRASNE, S. 1980. Interactions of voltage-sensing dyes with membranes. II. Spectrophotometric and electrical correlates of cyanine-dye adsorption to membranes. *Biophys. J.* **30**:000–000.

LÄUGER, P., and B. NEUMCKE. 1973. Theoretical analysis of ion conductance in lipid bilayer membranes. *In* Membranes—A Series of Advances. G. Eisenman, editor. Marcel Dekker, Inc., New York. **2**:1–50.

LEBLANC, O.H., Jr. 1971. The effect of uncouplers of oxidative phosphorylation on lipid bilayer membranes: carbonylcyanide-m-chorophenyl-hydrazone. *J. Membr. Biol.* **4**:227–51.

MCLAUGHLIN, S. 1972. The mechanism of action of DNP on phospholipid bilayer membranes. *J. Membr. Biol.* **9**:361–372.

MCLAUGHLIN, S. 1975. Local anaesthetics and electrical properties of phospholipid bilayer membranes. *In* Molecular Mechanism of Anaesthesia. B.R. Fink, editor. *Progr. Anaesthesiol.* Raven Press, New York. **1**:193–200.

MCLAUGHLIN, S. 1977. Electrostatic potentials at membrane-solution interfaces. *Curr. Top. Membranes Transp.* **9**:71–144.

MCLAUGHLIN, S., and H. HARARY. 1976. The hydrophobic adsorption of charged molecules to bilayer membranes: a test of the applicability of the Stern equation. *Biochemistry.* **15**:1941–1948.

MCLAUGHLIN, S., G. SZABO, and G. EISENMAN. 1971. Divalent ions and the surface potential of charged phospholipid membranes. *J. Gen. Physiol* **58**:667–687.

MCLAUGHLIN, S., G. SZABO, G. EISENMAN, and S. CIANI. 1970. Surface charge and the conductance of phospholipid membranes. *Proc. Natl. Acad. Sci. U.S.A.* **67**:1268–1275.

NEUMCKE, B., and E. BAMBERG. 1975. The action of uncouplers on lipid bilayer membranes. *In* Membranes—A Series of Advances. G. Eisenman, editor. Marcel Dekker, Inc., New York. **3**:215–253.

SMEJTEK, P., K. HSU, and W.H. PERLMAN. 1976. Electrical conductivity in lipid bilayer membranes induced by pentachlorophenol. *Biophys. J.* **16**:319–336.

SZABO, G., G. EISENMAN, R. LAPRADE, S. CIANI, and S. KRASNE. 1973. Experimentally observed effects of carriers on the electrical properties of bilayer membranes—equilibrium domain. *In* Membranes—A Series of Advances. G. Eisenman, editor. Marcel Dekker, Inc., New York. **2**:179–328.

WAGGONER, A. 1976. Optical probes of membrane potential. *J. Membr. Biol.* **27**:317–334.

WAGGONER, A.S., C-H. WANG, and R.L. TOLLES. 1977. Mechanism of potential-dependent light absorption changes of lipid bilayer membranes in the presence of cyanine and oxonol dyes. *J. Membr. Biol.* **33**:109–140.

WHITE, S. H. 1970. A study of lipid bilayer stability using precise measurements of specific capacitance. *Biophys. J.* **10**:1127–1148.